Journal of Metals, Materials and Minerals, 37(1), e2562, 2027

ZnO-enhanced PVA/HPMC electrospun fibers as multifunctional wound dressing materials

Kyi Pyar MIN LWIN[1], Gasidit PANOMSUWAN[1], Amornrat LERWORASIRIKUL[1], Nattapol CHAIMONGKOL[2], Ingorn KIMKONG[2], Prakit SUKYAI[3], Chatchawal WONGCHOOSUK[4], Kiadtisak SAENBOONRUANG[5], and Oratai JONGPRATEEP[1*]

[1] *Department of Materials Engineering, Faculty of Engineering, Kasetsart University, 50 Ngamwongwan Road, Chatuchak, Bangkok, 10900, Thailand*
[2] *Department of Microbiology, Faculty of Science, Kasetsart University, 50 Ngamwongwan Road, Chatuchak, Bangkok, 10900, Thailand*
[3] *Department of Biotechnology, Faculty of Agro-Industry, Kasetsart University, 50 Ngamwongwan Road, Chatuchak, Bangkok, 10900, Thailand*
[4] *Department of Physics, Faculty of Science, Kasetsart University, 50 Ngamwongwan Road, Chatuchak, Bangkok, 10900, Thailand*
[5] *Department of Applied Radiation and Isotopes, Faculty of Science, Kasetsart University, 50 Ngamwongwan Road, Chatuchak, Bangkok, 10900, Thailand*

***Corresponding author e-mail**: fengotj@ku.ac.th

Received date:
11 November 2025
Revised date:
18 March 2026
Accepted date:
29 June 2026

Keywords:
Nanocomposite fibrous mats;
Electrospinning technique;
Wound exudate management;
Antibacterial performance;
Mechanical properties

Abstract

Electrospun fibers are highly promising for wound dressings due to their high surface area, porosity, and capacity to carry bioactive agents. In this study, polyvinyl alcohol (PVA)/hydroxypropyl methylcellulose (HPMC)/Zinc Oxide (ZnO) nanocomposite fibrous mats were developed for wound healing applications. ZnO nanoparticles synthesized via a solution combustion method were successfully incorporated into the polymer matrix and electrospun onto nonwoven fiber paper. X-ray diffraction (XRD) and Fourier transform infrared spectroscopy (FTIR) confirmed ZnO integration and enhanced polymer-nanoparticle interactions. Atomic force microscopy revealed increased surface roughness, while scanning electron microscopy confirmed that ZnO incorporation maintained uniform, bead-free fibers with only a slight increase in average fiber diameter, suggesting improved interactions with wound exudates and bacteria. Mechanical testing revealed substantial enhancements: tensile strength increased from 3.93 ± 0.23 MPa to 10.15 ± 1.02 MPa, Young's modulus increased from 0.97 ± 0.18 MPa to 1.91 ± 0.33 MPa, and elongation at break increased from 10.60% to 18.85%, indicating improved flexibility and toughness. The contact angle ranged from 18.22° to 43.15°, showing balanced hydrophilicity, while the swelling ratio increased from 22.14 ± 3.27% to 78.82 ± 1.55%, supporting effective exudate absorption. Antibacterial activity was enhanced, with inhibition zones expanding from 9.00 ± 1.27 mm to 13.00 ± 0.79 mm for *E. coli* and from 13.75 ± 0.65 mm to 17.88 ± 0.25 mm for *S. aureus*. These findings demonstrate that PVA/HPMC/ZnO nanocomposite fibrous mats combine enhanced mechanical strength, moisture management, and antibacterial performance, highlighting their strong potential for advanced wound dressing applications.

1. Introduction

The skin acts as the body's primary protective barrier, shielding internal tissues from environmental threats and microbial infections. However, injuries such as cuts, burns, and ulcers compromise this defense, increasing susceptibility to bacterial contamination and delaying the wound healing process. Chronic wounds, in particular, pose significant medical challenges due to prolonged healing times and the risk of biofilm formation by pathogenic bacteria like *Staphylococcus aureus* and *Escherichia coli*. These biofilms create a protective matrix that shields bacteria from antibiotics and the immune system, leading to persistent infections that can result in systemic inflammation, delayed tissue regeneration, and even sepsis [1]. As a result, there is an urgent need for advanced wound dressing materials that not only support the healing process but also provide effective antimicrobial protection.

Moreover, wound healing is a complex, multi-phase process involving hemostasis, inflammation, proliferation, and tissue remodelling [2]. For optimal outcomes, wound dressings must maintain a moist environment, prevent infections, and promote tissue regeneration. Traditional dressings like cotton gauze offer basic protection but lack bioactive functionality. In contrast, advanced dressings such as hydrogels, polymeric films, and nanocomposites provide moisture retention, exudate absorption, controlled drug release, and antimicrobial activity [3].

An ideal wound dressing should be biocompatible to avoid immune responses [4], maintain moisture balance while allowing gas exchange [5], exhibit antimicrobial activity to prevent infections [6], and offer mechanical stability and flexibility to conform to various wound sites [7]. Effective exudate management is also crucial, as both excessive moisture and desiccation can impair healing [8].

The choice of polymer matrix plays a critical role. Polyvinyl alcohol (PVA) is widely used for its film-forming ability, hydrophilicity, biocompatibility, and mechanical strength [9]. It retains moisture, promotes cell proliferation, and can be electrospun into uniform nanofibers that enhance healing [10]. To further improve mechanical stability and moisture management, Hydroxypropyl methylcellulose (HPMC), a biocompatible, hydrophilic cellulose derivative with excellent film-forming and moisture-retention properties, was incorporated into the nanofiber matrix. Its structural similarity to the extracellular matrix (ECM) also supports tissue regeneration and fiber durability [11].

Electrospinning is a promising technique for fabricating advanced wound dressings, producing nanofibrous scaffolds that mimic the ECM, promote cell adhesion, and enable efficient gas exchange and moisture retention. These fibers also allow the incorporation of bioactive agents, enabling the controlled delivery of therapeutic agents [12].

Among antimicrobial agents, zinc oxide (ZnO) nanoparticles are particularly attractive due to their broad-spectrum antibacterial activity, biocompatibility, and wound-healing potential. ZnO combats bacteria through multiple mechanisms: generating reactive oxygen species (ROS) that damage cellular components [13], disrupting membrane integrity [14], releasing Zn^{2+} ions that interfere with bacterial metabolism [15], and inhibiting biofilm formation [16]. These properties make ZnO a valuable addition to enhancing the functionality of wound dressing materials.

In recent years, a number of studies have explored the integration of metal and metal-oxide nanoparticles into polymeric or biopolymeric wound dressing systems to impart antibacterial functionality, improve mechanical performance, and accelerate healing. For example, a green-synthesized ZnO-loaded keratin/sodium-alginate biopolymeric mat demonstrated enhanced antimicrobial and wound-healing properties, supporting the use of ZnO within natural polysaccharide-based dressings [17]. Similarly, a flexible biopolymeric chitosan/agarose scaffold reported recently [18] incorporated metal-oxide nanofillers and showed improved conformability and bacterial inhibition. Furthermore, recent reviews of metal- and metal-oxide nanoparticle composite formulations for wound dressings including silver (Ag), cerium dioxide (CeO_2), titanium dioxide (TiO_2), and ZnO highlight their multifunctional role in balancing moisture control, antimicrobial activity, and mechanical support [19]. These studies emphasize the potential of metal oxide-based nanocomposites and validate the rationale for incorporating ZnO into polymeric electrospun matrices to achieve multifunctional wound dressings. However, the combined optimization of mechanical robustness, moisture management, and antibacterial performance in a single electrospun system remains challenging.

In this study, PVA/HPMC/ZnO nanocomposite fibrous mats were fabricated using electrospinning and evaluated for their potential as multifunctional wound dressing materials. ZnO nanoparticles, synthesized via the solution combustion method, were incorporated into the PVA/ HPMC matrix to impart antimicrobial functionality. The electrospinning process was optimized to achieve uniform fiber formation directly onto a nonwoven fiber paper, producing mats with enhanced crystallinity, tailored surface roughness, balanced hydrophilicity and water resistance. The structural, mechanical, and functional properties of the mats were thoroughly characterized, focusing on crystallinity, surface morphology, wettability, and water stability. Additionally, the antimicrobial performance against common wound pathogens (*E. coli* and *S. aureus*) was significantly improved with ZnO incorporation. These findings position the ZnO-enhanced PVA/HPMC electrospun fibers as a promising platform for next-generation wound dressings, offering strong antibacterial activity, excellent structural integrity, and optimal moisture management for enhanced wound healing outcomes.

2. Experimental

2.1 Synthesis and characterization of ZnO particles

ZnO nanoparticles were synthesized using the solution combustion method. Zinc nitrate hexahydrate was dissolved in deionized water, followed by the addition of glycine as a fuel to form a homogeneous precursor solution. The solution was then heated in a glass beaker placed on a hot plate under ambient conditions. Upon reaching approximately 400°C, a self-sustained combustion reaction was initiated directly within the beaker, resulting in the formation of ZnO nanoparticles. To improve purity and crystallinity, the as-synthesized powder was further calcined at 500°C and subsequently ground into a fine powder for incorporation into the polymer matrix, as illustrated in Figure 1.

Phase identification of the powder synthesized through the solution combustion method was carried out using X-ray diffraction (XRD, Empyrean, Malvern Panalytical, UK) over a 2θ range of 20° to 80° with a step size of 0.02°**.** To examine the morphology and particle size, a scanning electron microscope (SEM, Hitachi SU3500) was utilized.

2.2 Synthesis and characterization of PVA/HPMC/ZnO electrospun fibres

For the polymer matrix, a 10% (w/v) PVA (polyvinyl alcohol, Sigma-Aldrich, Mw 85,000 to 124,000, 99%) solution was prepared by dissolving PVA in deionized water at 90°C, while a 3% (w/v) HPMC solution (hydroxypropyl methylcellulose, METHOCEL™ F4M) was prepared by dissolving HPMC at 60°C. Equal volumes of both solutions were mixed and stirred at room temperature for 6 h to form a homogeneous blend. Citric acid corresponding to 10% (w/w) of the total polymer weight was then added as a crosslinking agent to enhance structural stability through interactions with hydroxyl groups in PVA and HPMC. The mixture was then stirred for an additional 2 h to ensure proper crosslinking, followed by sonication for 30 min to ensure uniform dispersion of all components.

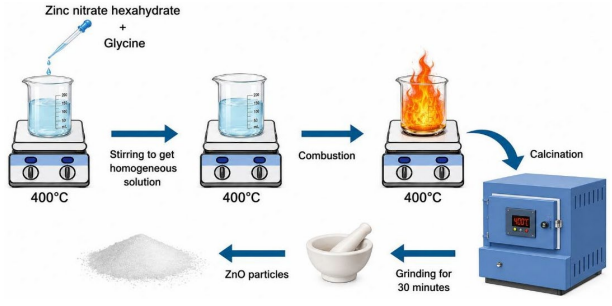


Figure 1. Schematic of ZnO nanoparticle synthesis via solution combustion. The precursor solution was heated in a glass beaker on a hot plate (400°C), where combustion occurs to form ZnO, followed by calcination and grinding.

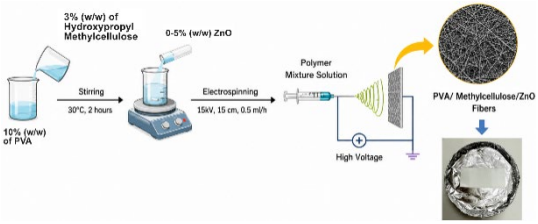


Figure 2. Schematic illustration of PVA/HPMC/ZnO electrospun fiber fabrication.

ZnO nanoparticles were pre-dispersed in deionized water at the desired concentrations (0.5% to 5% (w/w)) using probe ultrasonication for 15 min to ensure uniform distribution, followed by magnetic stirring for 1 h to achieve stable dispersion. The resulting ZnO suspensions were added slowly to the PVA–HPMC–citric acid mixture using a pipette over several min under continuous stirring to promote homogeneous nanoparticle incorporation. The resulting suspension was subsequently probe ultrasonicated for 30 min to minimize nanoparticle agglomeration and allowed to stand undisturbed for 2 h to remove entrapped air bubbles.

Prior to electrospinning, the homogeneous ZnO-loaded polymer suspension was again sonicated to ensure stable dispersion of the nanoparticles. Electrospinning was conducted under optimized conditions: an applied voltage of 15 kV, a tip-to-collector distance of 15 cm, and a feed rate of 0.5 mL·h^{-1} for 6 h. The obtained nanofibrous mats were collected on aluminum foil and subsequently heat-treated in an oven at 120°C for 1 h to promote citric acid-induced crosslinking. For physicochemical characterization, the nanofiber mats were stored under clean, sealed conditions. For antibacterial testing, all experiments were conducted under clean and controlled laboratory conditions, with laboratory ware disinfected using 70% ethanol prior to use. A schematic illustration of the overall fabrication process is presented in Figure 2.

The synthesized PVA/HPMC/ZnO electrospun fibers were characterized to evaluate their composition, structure, and physical properties. Phase analysis was carried out using X-ray diffraction (XRD, Empyrean, Malvern Panalytical, UK) with a scanning range of 5° to 80° (2θ), a scan rate of 3° per minute, and a step size of 0.02°. The surface morphology and elemental composition of the fibers were examined using scanning electron microscopy (SEM, SU3500, Hitachi, Japan) and the average fiber diameter was determined using ImageJ software. Functional groups present in the electrospun fibers were identified by Fourier transform infrared spectroscopy (FTIR; Bruker, Alpha), with spectra collected in the range of 500 cm^{-1} to 4000 cm^{-1}.

The swelling behavior of the wound dressing samples was evaluated using a phosphate-buffered saline (PBS) absorption assay. Briefly, the samples were cut into square pieces (1 cm × 1 cm) and freeze-dried to a constant weight. The initial dry weight of each sample (W_d) was measured using an analytical balance. The samples were then immersed in PBS solution (pH 7.4) and incubated at 37°C for 24 h. After incubation, the samples were removed, gently blotted with filter paper to eliminate excess surface liquid, and immediately weighed to obtain the swollen weight (W_s). The swelling ratio was calculated using the following equation:

$$\text{Swelling ratio (\%)} = \frac{W_s - W_d}{W_d} \times 100$$

Mechanical properties of the electrospun fibrous mats were evaluated using a universal testing machine (UTM, H50KS) in accordance with ASTM D882. Rectangular specimens (2 cm × 10 cm) were tested at room temperature with a gauge length of 50 mm and a crosshead speed of 5 mm·min^{-1}. The specimen thickness was measured at multiple locations and averaged to determine the initial cross-sectional area. Tensile strength, Young's modulus, and elongation at break were calculated from the resulting stress–strain curves. At least three specimens (n = 3) were tested for each sample.

The surface wettability of the electrospun fibrous mats was evaluated using a contact angle goniometer (DM-CE1, Kyowa Interface Science Co., Ltd., Saitama, Japan) in accordance with ASTM D7334. Samples (1 cm × 1 cm) were fixed onto a glass slide, and a 3 µL droplet of deionized water was deposited onto the sample surface at room temperature. The contact angle was recorded within 5 s using an optical imaging system. Measurements were performed at five different locations on each sample, and the average value was reported.

For contact angle measurements, three independent measurements were performed for each sample (n = 3). In addition, statistical analysis was conducted to evaluate the influence of ZnO concentration on the wettability behavior of the electrospun fibers. Pairwise comparisons between adjacent ZnO concentrations (0% to 0.5%, 0.5% to 1%, 1% to 2%, 2% to 3%, and 3% to 5% (w/w)) were performed using one-way ANOVA in Microsoft Excel, with statistical significance defined as $p < 0.05$.

The agar well diffusion method was employed to assess the antibacterial activity of the samples. Briefly, each bacterial suspension was uniformly spread onto Mueller Hinton Agar (MHA) plates using sterile cotton swabs in three directions to ensure even distribution. Wells of 6 mm diameter were aseptically punched into the agar using a sterile cork borer. Subsequently, 20 µL of the sample extract at a concentration of 200 mg·mL^{-1} was carefully loaded into each well. The plates were then incubated at 37°C for 24 h. After incubation, the zones of inhibition were observed and measured in mm to evaluate antibacterial efficacy.

Gentamicin (10 µg·disc^{-1}) was used as the positive control, while the ZnO-free PVA/HPMC matrix (blank) served as the negative control. All tests were performed in triplicate to ensure accuracy and reproducibility.

3. Results and discussion

3.1 Structural and morphological features of ZnO particles

The XRD pattern of the powder synthesized by the solution combustion technique, shown in Figure 3, confirms the presence of a single-phase wurtzite structure in the ZnO nanoparticles (ZnO NPs). The observed diffraction peaks at 31.74°, 34.4°, 36.23°, 47.51°, 56.55°, 62.82°, 66.32°, 67.89°, 69.03°, 72.52°, and 76.89° corresponded to the (100), (002), (101), (102), (110), (103), (200), (112), (201), (004), and (202) crystallographic planes, respectively [20,21]. The sharp, well-defined peaks indicate a highly crystalline single-phase material. The average crystallite size of the ZnO NPs, determined using the Scherrer equation, was approximately 50 nm.

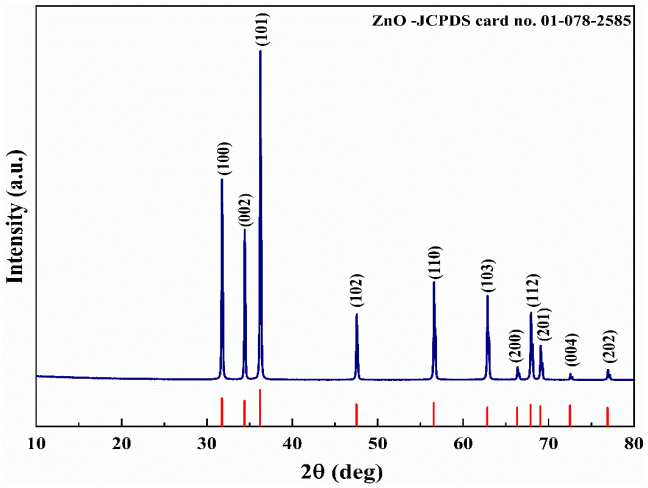


Figure 3. XRD pattern of synthesized ZnO powders.

The morphology of the synthesized ZnO nanoparticles was analyzed using SEM. The SEM image, shown in Figure 4, reveals an irregular, faceted morphology with a small proportion of rod-shaped nanoparticles. ImageJ analysis indicated an average particle size of 60 nm. The energy-dispersive X-ray (EDS) spectrum confirms the presence of zinc and oxygen, validating the composition of the ZnO nanoparticles.

This unique morphology offers several advantages for antimicrobial applications in wound dressing, which are crucial for effective antimicrobial properties by increasing contact with bacterial cells and promoting stronger antibacterial activity. Additionally, the irregular, faceted structure enhances the interaction of the ZnO nanoparticles with surrounding substances, further improving their ability to disrupt bacterial membranes and eliminate bacteria. These characteristics make ZnO nanoparticles highly suitable for wound dressing applications, where their ability to prevent infection, support healing, and maintain a clean wound environment is crucial [22–24].

The surface properties of ZnO nanoparticles were analyzed using N_2 adsorption-desorption measurements based on the Brunauer-Emmett-Teller (BET) method. The isotherm reveals a combination of Type II and Type IV isotherms with an H3 hysteresis loop, indicating the predominant presence of meso- and macropores [25]. The mesoporous structure of ZnO nanoparticles, with pores in the range of 2 nm to 50 nm and a pore volume of 0.007944 $cm^3 \cdot g^{-1}$, may contribute to antibacterial activity by facilitating adsorption and enhancing interactions with bacterial cells. The increased porosity allows for better trapping of microorganisms and more effective antibacterial action. Furthermore, the mesopores can serve as channels for the diffusion of reactive oxygen species (ROS), such as hydroxyl radicals and hydrogen peroxide, which disrupt bacterial membranes and kill bacteria [26].

Although SEM analysis indicated that the ZnO nanoparticles possess a primary particle size of approximately 60 nm typically associated with a high specific surface area the BET results revealed a relatively low surface area of 5.48 $m^2 \cdot g^{-1}$. This apparent discrepancy can be attributed to particle agglomeration, as observed in the SEM images, where individual nanoparticles tend to cluster into larger aggregates. Such aggregation reduces the effective external surface area and limits the accessibility of pores for nitrogen adsorption during BET analysis. Therefore, while the intrinsic nanoscale size of the ZnO particles suggests a high theoretical surface area, the actual measured BET surface area reflects the aggregated state of the particles rather than their primary size. This highlights the importance of dispersion in determining the accessible surface area and suggests that further strategies to minimize agglomeration could enhance the surface-related properties of the material.

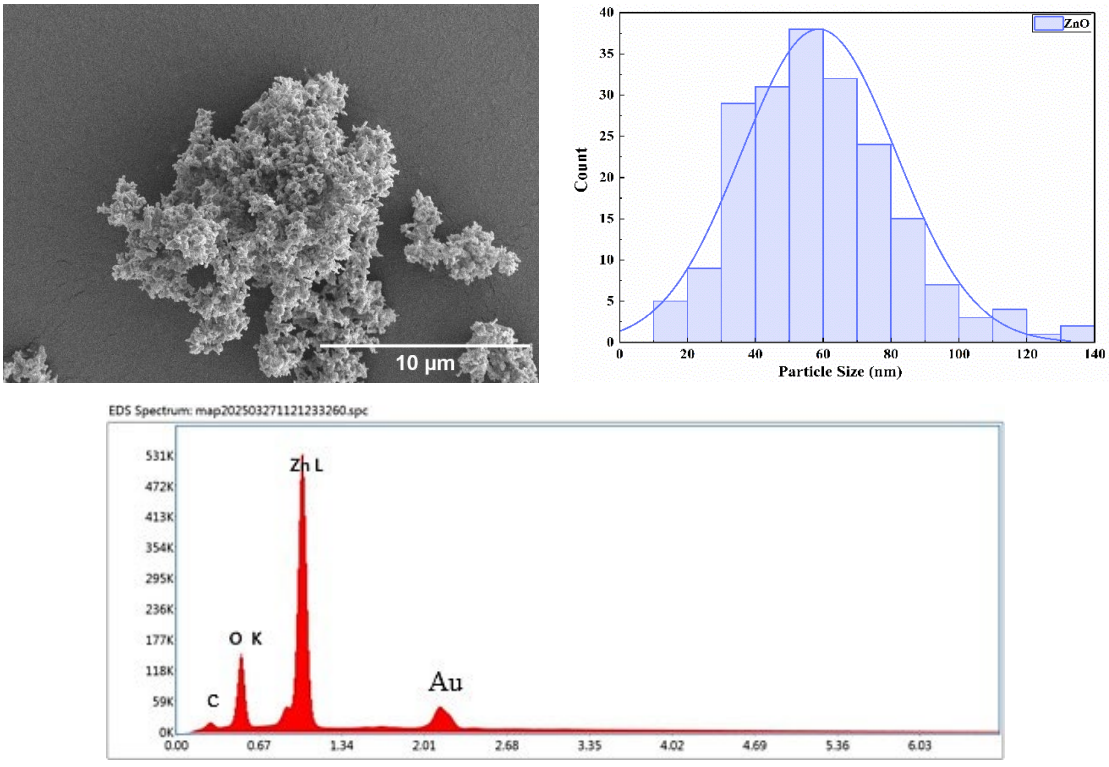


Figure 4. Morphology, particle size distribution and elemental analysis of ZnO powders.

To address the issue of agglomeration, the ZnO nanoparticles were dispersed in the PVA/HPMC precursor solution before electrospinning. This approach helps reduce particle agglomeration, maintain their individual surface area, and improve their antibacterial efficiency. By optimizing dispersion, the mesoporous characteristics and accessible surface area of the ZnO nanoparticles can be better preserved, thereby enhancing their interactions with bacterial cells and improving their antibacterial performance.

3.2 Characteristics of PVA/HPMC/ZnO electrospun fibers

3.2.1 Structural and chemical characterization of PVA/HPMC/ZnO electrospun fibers

XRD analysis was conducted to investigate the structural characteristics of pure PVA, HPMC, their composites, and ZnO-loaded PVA/HPMC composites. Pure PVA, as shown in Figure 6, exhibits a broad peak cantered around $2\theta = 19.5°$, indicative of its predominantly amorphous nature, with a minor shoulder peak near 22° and a small broad signal observed around 40°. These features reflect the semi-crystalline character of PVA and contribute to its flexibility an essential property for wound dressing applications. HPMC, in comparison, displayed a single broad peak at approximately $2\theta = 21.5°$, consistent with its amorphous structure. The PVA/HPMC composite showed a merged and broadened peak near $2\theta = 20°$, suggesting good miscibility and structural compatibility between the two polymer [27]. Upon incorporation of ZnO nanoparticles (0% to 5% (w/w)), distinct diffraction peaks appeared at 2θ values of 31.7°, 34.4°, and 36.2°, corresponding to the (100), (002), and (101) planes of the hexagonal wurtzite ZnO structure [21]. These peaks became increasingly prominent with higher ZnO content, confirming not only the preservation of ZnO's crystalline form but also the successful incorporation of ZnO nanoparticles into the PVA/HPMC polymer matrix. This structural integration is critical, as the retained crystallinity of ZnO directly contributes to the composite's antibacterial performance and UV-blocking capacity key attributes for effective wound healing applications.

In addition to the appearance of ZnO diffraction peaks, the broad polymer diffraction feature centered around $2\theta \approx 20°$ remained present in all ZnO-loaded samples, indicating that the semi-crystalline nature of the PVA/HPMC matrix was largely preserved after nanoparticle incorporation. No substantial shift in the position of this broad peak was observed, suggesting that ZnO addition did not significantly alter the crystalline structure of the polymer blend. However, a gradual reduction in the relative prominence of the polymer peak was observed with increasing ZnO loading. This behavior may be attributed to the increasing contribution of the highly crystalline ZnO phase, which partially masks the broad polymer diffraction signal. Furthermore, interactions between ZnO nanoparticles and the hydroxyl groups of PVA and HPMC may slightly restrict polymer chain mobility, influencing local chain organization while maintaining the overall semi-crystalline character of the matrix. These results indicate that ZnO nanoparticles reinforce the composite through the introduction of an additional crystalline phase without disrupting the fundamental structural characteristics of the PVA/HPMC polymer network.

Fourier-transform infrared (FTIR) spectroscopy was employed to identify the functional groups present in pure PVA, HPMC, and their ZnO-containing nanocomposite. The FTIR spectrum of PVA, as shown in Figure 7, exhibits a broad absorption band between 3200 cm^{-1} and 3500 cm^{-1}, characteristic of O–H stretching vibrations resulting from extensive hydrogen bonding. A sharp peak near 2900 cm^{-1} corresponded to C–H stretching of methylene groups, while a weak band around 1730 cm^{-1} indicated residual C=O stretching from incompletely hydrolyzed acetate groups. Additionally, a peak at 1410 cm^{-1} was assigned to C–H bending and O–H deformation vibrations, and strong absorptions between 1080 cm^{-1} and 1140 cm^{-1} confirmed the presence of C–O stretching associated with alcohol groups [28].

The HPMC spectrum displayed similar features, including a broad O–H stretching band at 3300 cm^{-1} to 3400 cm^{-1} and a prominent C–H stretching peak near 2900 cm^{-1}. A pronounced band around 1140 cm^{-1} was attributed to C–O–C asymmetric stretching of β-1,4-glycosidic linkages, while additional C–O stretching peaks appeared between 1020 cm^{-1} and 1060 cm^{-1}. A distinct peak near 895 cm^{-1} further confirmed the presence of β-glycosidic bonds characteristic of the HPMC backbone [29,30].

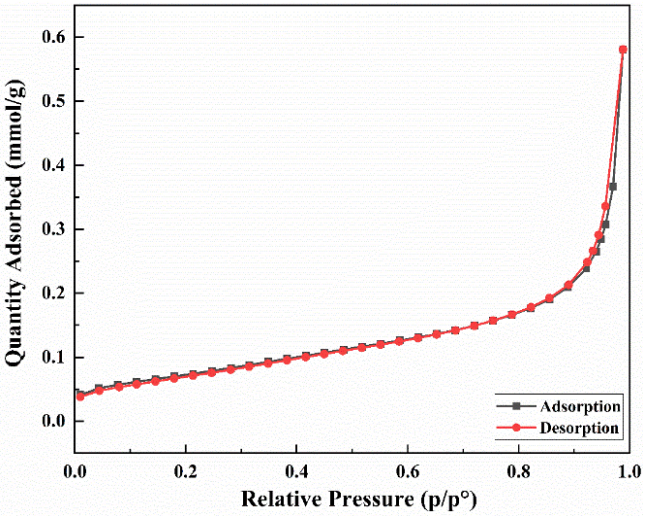


Figure 5. N_2 adsorption–desorption isotherm of ZnO.

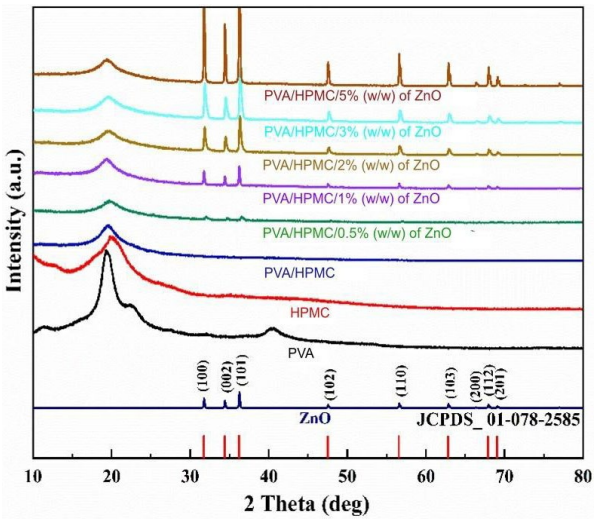


Figure 6. XRD diffraction patterns of PVA/HPMC polymeric fibers with varying ZnO loadings.

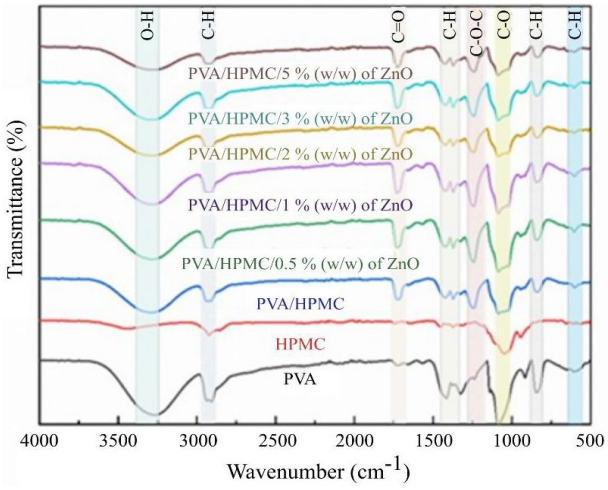


Figure 7. FTIR spectra of (a) PVA, (b) HPMC, (c) PVA/HPMC/0% (w/w) of ZnO, (d) PVA/HPMC/0.5% (w/w) of ZnO, (e) PVA/HPMC/1% (w/w) of ZnO, (f) PVA/HPMC/2% (w/w) of ZnO, (g) PVA/HPMC/3% (w/w) of ZnO, and (h) PVA/HPMC/5% (w/w) of ZnO.

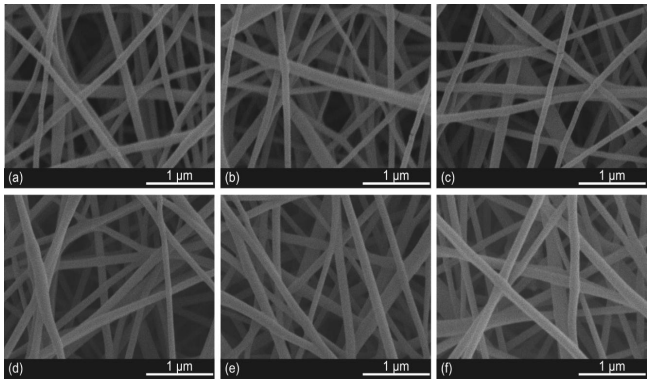


Figure 8. SEM images of (a) PVA/HPMC, (b) PVA/HPMC/0.5% (w/w) of ZnO, (c) PVA/HPMC/1% (w/w) of ZnO, (d) PVA/HPMC/2% (w/w) of ZnO, (e) PVA/HPMC/3% (w/w) of ZnO, and (f) PVA/HPMC/5% (w/w) of ZnO.

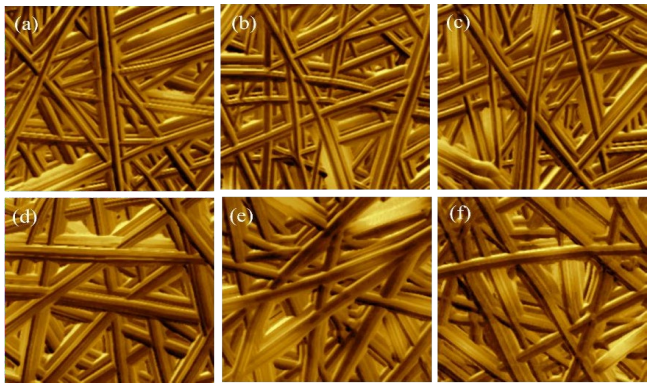


Figure 9. AFM images of (a) PVA/HPMC, (b) PVA/HPMC/0.5% (w/w) of ZnO, (c) PVA/HPMC/1% (w/w) of ZnO, (d) PVA/HPMC/2% (w/w) of ZnO, (e) PVA/HPMC/3% (w/w) of ZnO, and (f) PVA/HPMC/5% (w/w) of ZnO.

3.2.2 Morphological and topographical analysis of PVA/HPMC/ZnO electrospun fibers

The PVA/HPMC composite spectrum retained characteristic peaks from both poly-mers, confirming effective blending. Notably, the C=O stretching band near 1700 cm^{-1} was more intense than in the individual components, suggesting enhanced hydrogen bonding or possible esterification between hydroxyl groups of PVA and HPMC. This implies strong inter-molecular interactions and good compatibility within the composite matrix [31].

FTIR analysis further confirmed the successful incorporation of ZnO nanoparticles into the PVA/HPMC blend. Characteristic peaks corresponding to O–H, C–H, C=O, and C–O stretching vibrations remained clearly identifiable, exhibiting only slight shifts after ZnO addition. These minimal spectral changes indicate that the chemical integrity of the PVA/HPMC matrix was largely preserved, maintaining its biocompatibility and moisture-handling properties.

Collectively, these structural and chemical characterizations demonstrate that the nanocomposite fibers retain the desirable flexibility, biocompatibility, and moisture management of the PVA/HPMC matrix, while effectively incorporating ZnO's antimicrobial and UV-resistant functionalities. This synergy of properties makes the material highly suitable for wound dressing applications, providing a protective, antibacterial, and healing-conducive environment that promotes tissue regeneration and prevents infection.

SEM analysis revealed uniform, bead-free nanofibers across all samples, indicating successful optimization of the electrospinning process a critical factor for ensuring consistent wound coverage and mechanical integrity. The average fiber diameter increased slightly from 122 nm (0% (w/w) of ZnO) to 147 nm (5% (w/w) of ZnO) with the incorporation of ZnO na-noparticles. This diameter range closely mimics the architecture of the natural extracellular matrix (ECM), which is advantageous for promoting cell adhesion, migration, and proliferation [32].

Atomic force microscopy (AFM) analysis, shown in Figure 9, demonstrated an increase in surface roughness with higher ZnO content, as indicated by the rising R_a values from 0.08918 µm for the pure sample to 0.2018 µm for the 5% (w/w) ZnO-loaded sample. This enhanced nanoscale roughness not only increases the surface area available for cell-fiber interactions but also plays a crucial role in modulating cellular responses. A moderately rough surface has been shown to promote fibroblast attachment and proliferation, while simultaneously reducing bacterial adhesion making it ideal for wound healing applications [33].

In addition, the observed nanoscale roughness ($R_a \approx 0.20$ µm) falls within the range reported to influence cell material interactions through extracellular matrix (ECM) mimicking surface cues. Native ECM exhibits a hierarchical architecture spanning nano to microscale fea-tures, which plays a critical role in regulating cell adhesion, migration, and proliferation. Surfaces with controlled nanoscale roughness can enhance the adsorption and spatial organization of adhesion-related proteins, such as fibronectin and vitronectin, thereby promoting integrin-mediated cell attachment and focal adhesion formation. Furthermore, the combination of fibrous morphology and surface roughness in electrospun mats provides a biomimetic microenvironment that closely resembles the structural complexity of natural tissue. Previous studies have demonstrated that nanoscale topographical features can regulate cell behavior, including adhesion, spreading, and differentiation, through mechanotransduction pathways [34]. Similarly, the importance of ECM-mimicking complexity in biomaterial design has been high-lighted as a key factor in enhancing cellular responses and tissue regeneration

[35]. Although direct biological evaluation was not performed in this study, the measured roughness and fibrous architecture suggest that the developed PVA/HPMC/ZnO mats may provide favorable ECM-like cues for supporting tissue regeneration.

Collectively, the SEM and AFM results indicate that the fabricated PVA/HPMC/ZnO nanofibrous mats possess key morphological and surface characteristics desirable for wound dressings: uniform fiber formation for structural reliability, biomimetic fiber dimensions to support cellular activities, effective ZnO integration for antimicrobial action, and optimized surface roughness to enhance tissue regeneration.

Although SEM observations confirmed the formation of uniform nanofibrous structures and the successful incorporation of ZnO was verified by XRD, FTIR, and antibacterial perfor-mance, further investigation using SEM–EDX elemental mapping could provide additional in-sight into the spatial distribution and dispersion homogeneity of ZnO nanoparticles throughout the electrospun fiber matrix.

3.2.3 Wettability and functional implications of PVA/HPMC/ZnO electrospun fibers

The contact angle measurements offer valuable insights into the wettability and moisture control of the PVA/HPMC/ZnO nano-composite fibers for wound dressing applications. A contact angle between 40° and 70° strikes the ideal balance for moisture retention, which is crucial for wound healing [36]. This range supports cell migration, proliferation, and angio-genesis, while allowing for exudate absorption without excessive fluid loss, maintaining an optimal moisture balance.

A contact angle lower than 30° indicates high hydrophilicity, which may lead to exces-sive fluid absorption, potentially disrupting the moisture balance and causing the dressing to become too wet. This could lead to maceration of the wound, hindering healing. As the contact angle approaches 70°, the material becomes more hydrophobic, enhancing its barrier properties to prevent excessive moisture absorption and protect the wound from contaminants, thus re-ducing infection risk while still maintaining necessary moisture for healing. However, a contact angle above 70° results in excessive hydrophobicity, which may repel wound exudate, dry out the wound, and delay healing. It can also impede cell migration and proliferation, slowing tissue regeneration. Maintaining an optimal contact angle is crucial for effective healing and infection prevention.

In this study, the addition of ZnO in the range of 1% to 5% (w/w) increased the contact angle from 18.22° to 43.15°, indicating a gradual transition from highly hydrophilic to moderately hydrophilic behavior. Although some samples exhibited contact angle values below the commonly reported range of 40° to 70° for balanced moisture management, such high hydrophilicity may still be advantageous for wound dressings intended for low- to moderate-exudate wounds, where efficient fluid uptake and maintenance of a moist healing environment are desirable.

The observed wettability characteristics suggest that the developed electrospun mats are capable of absorbing wound exudate while maintaining adequate surface moisture, which is beneficial for supporting tissue regeneration and wound healing. The observed increase in hydrophobicity is likely due to enhanced surface roughness and reduced exposure of hydrophilic groups due to ZnO interactions.

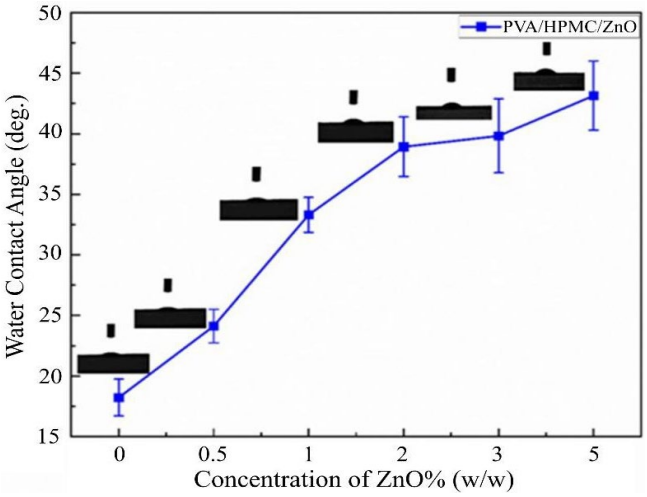


Figure 10. Wetting behaviours of PVA/HPMC/ZnO fibers with varying ZnO concentrations: 0%, 0.5%, 1%, 2%, 3% and 5% (w/w).

The progressive increase in contact angle with ZnO incorporation suggests improved control over moisture absorption while preserving sufficient wettability for cell attachment and proliferation. Therefore, ZnO incorporation provides a means of tailoring the surface wettability of the electrospun mats, enabling a balance between fluid management, antimicrobial functionality, and wound-healing support.

Statistical analysis further revealed that the increase in contact angle was significant between 0% and 2% (w/w) ZnO loading ($p < 0.05$), whereas no statistically significant differences were observed between 2% and 3% (w/w) ZnO or between 3% and 5% (w/w) ZnO ($p > 0.05$). This behavior suggests that the influence of ZnO on surface wettability becomes less pronounced at higher nanoparticle concentrations. At lower loadings, ZnO incorporation substantially modifies the surface characteristics of the electrospun fibers, including surface roughness and surface energy, resulting in measurable changes in wettability. However, beyond approximately 2% (w/w) ZnO, much of the accessible fiber surface may already be influenced by the presence of ZnO nanoparticles, such that additional ZnO contributes only limited further changes to the surface characteristics governing water–surface interactions. Furthermore, a fraction of the added nano-particles may become embedded within the fiber matrix, reducing their contribution to the effective surface exposed to the water droplet. Consequently, additional ZnO loading results in only marginal changes in contact angle, leading to the observed plateau-like behavior. This observation suggests that relatively low ZnO concentrations may be sufficient to achieve significant wettability modification, while further increases in ZnO loading provide diminishing effects on surface wetting behavior.

3.2.4 Swelling ratio analysis of PVA/HPMC/ZnO electrospun fibers

The swelling behavior of ZnO-incorporated PVA/HPMC electrospun fibers was investigated to evaluate their water absorption capacity a critical property for wound healing applications. Effective wound dressings must absorb excess exudate to prevent infection while retaining sufficient moisture to support cell proliferation and tissue regeneration. While swelling ratios for wound dressings are often

cited in the moderate range of 100% to 300%, particularly for highly exudative wounds, lower swelling ratios can still be highly effective for wounds with low to moderate exudate or for multifunctional dressings that prioritize other factors such as antimicrobial activity, flexibility, and conformability.

The reported swelling values correspond to measurements obtained after 24 h of immersion in PBS (pH 7.4) at 37°C. This immersion period was selected because 24 h soaking is widely used for evaluating the fluid absorption and swelling behavior of electrospun wound dressing materials and hydrophilic polymer systems under physiologically relevant conditions. Although swelling kinetics were not monitored at intermediate time points in the present study, the 24 h measurement provides a practical assessment of the water uptake capacity of the developed nanofibrous mats during prolonged exposure to an aqueous environment. Therefore, the reported values represent swelling ratios after 24 h of immersion rather than equilibrium swelling ratios.

As shown in Figure 11, the swelling capacity of the fibers increased with ZnO content, rising from 22.14 ± 3.27% (0% (w/w) of ZnO) to 78.82 ± 1.55% (5% (w/w) of ZnO). This trend indicates a strong correlation between ZnO incorporation and improved moisture uptake. Although the values remain below the conventional upper range, they are well-suited for low to moderately exuding wounds where over-swelling could lead to dressing breakdown or maceration of healthy tissue. Additionally, this level of swelling ensures sufficient moisture retention to maintain a moist healing environment an essential condition for optimal tissue regeneration.

Swelling in polymeric materials occurs as water molecules diffuse into the polymer matrix and interact with hydrophilic functional groups such as hydroxyl (–OH) groups in PVA and HPMC. These interactions promote chain expansion, facilitating water retention and increasing the overall swelling capacity. Contact angle measurements (as discussed earlier) revealed a moderate increase in surface hydrophobicity with rising ZnO content, which is attributed to enhanced surface roughness and partial shielding of hydrophilic groups. This hydrophobic effect, however, is primarily limited to the fiber surface and does not significantly impact the material's internal swelling behavior.

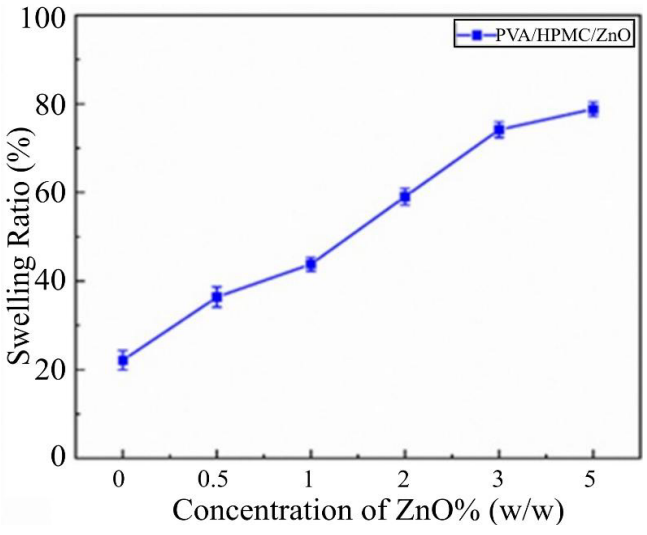


Figure 11. Swelling behavior of PVA/HPMC/ZnO fibers with varying ZnO concentrations: 0%, 0.5%, 1%, 2%, 3%, and 5% (w/w).

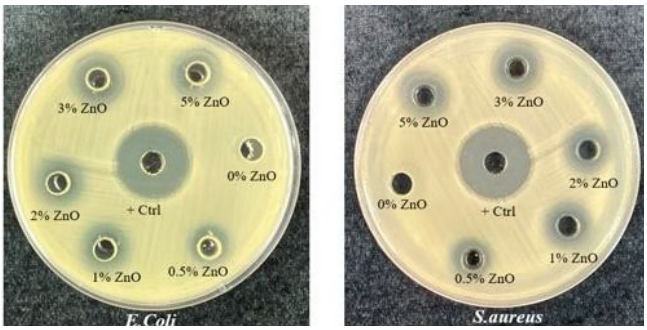


Figure 12. Photographs showing the antibacterial activity of PVA/HPMC based with (0% to 5% (w/w)) of ZnO against *E. coli* and *S. aureus.*

The bulk material remains hydrophilic, and the incorporation of ZnO nanoparticles may contribute to increased swelling through several mechanisms that improve moisture retention. ZnO's high surface area and polar nature may introduce additional hydrogen bonding sites within the fiber interior, and its intrinsic hydrophilicity may further support water diffusion throughout the matrix. As the fibers swell, they not only retain more moisture but also gain flexibility, enabling better conformability to the wound surface. This helps maintain intimate contact with the tissue, prevents brittleness or cracking, and provides a soft, cushioning effect that protects against mechanical irritation. Additionally, the absorbed fluid increases the dressing's ability to manage exudate without structural collapse or leakage, supporting both moisture balance and material stability over time. Thus, the combination of moderate surface hydrophobicity and enhanced internal swelling offers a dual-function behavior that is highly beneficial for wound dressings supporting infection prevention, tissue regeneration, and long-term mechanical integrity.

3.2.5 Antibacterial testing of PVA/HPMC/ZnO electrospun fibers

The antibacterial performance of PVA/HPMC fibers was assessed through zone-of-inhibition assays against Staphylococcus aureus and Escherichia coli (Figure 12 and Table 1). As anticipated, fibers without ZnO exhibited no inhibition zones, confirming the absence of inherent antibacterial properties in the base polymer matrix. In contrast, the incorporation of ZnO nanoparticles imparted significant antibacterial activity. At 0.5% (w/w) of ZnO, the fibers exhibited inhibition zones of 13.75 ± 0.65 mm against *S. aureus* and 9 ± 1.27 mm against *E. coli.* These zones increased with higher ZnO content, reaching 17.88 ± 0.25 mm and 13 ± 0.79 mm, respectively, at 5% (w/w). However, beyond 2% (w/w) ZnO, the rate of improvement became less pronounced, suggesting a saturation-like behavior in which further increases in ZnO loading provided only marginal enhancement in antibacterial performance, possibly due to nanoparticle agglomeration that reduces the effective surface area available for interaction with bacterial cells.

The antibacterial activity of ZnO nanoparticles has been widely attributed to several mechanisms reported in the literature, including the generation of reactive oxygen species (ROS), such as hydroxyl radicals (•OH), superoxide anions ($•O_2^-$), and hydrogen peroxide (H_2O_2), as well as the release of Zn^{2+} ions under physiological conditions. These species have been reported to damage bacterial cell membranes,

denature intracellular proteins, disrupt enzymatic activity, and induce DNA damage, ultimately leading to bacterial cell death. In addition, the nanoscale dimensions and intrinsic surface properties of ZnO nanoparticles facilitate close contact with bacterial cells, which may further enhance antibacterial activity. [20] Although these mechanisms are well documented in previous studies, ROS generation and Zn^{2+} release were not directly investigated in the present work. Therefore, they are discussed here as plausible mechanisms rather than experimentally verified processes.

ZnO-loaded fibers demonstrated stronger antibacterial activity against Gram-positive *S.aureus* than against Gram-negative *E.coli*. This is commonly observed due to the structural differences in bacterial cell walls Gram-positive bacteria have a thicker peptidoglycan layer but lack the protective outer membrane found in Gram-negative bacteria, making them more vulnerable to nanoparticle and ROS-induced damage.

In hydrated or physiological environments, the antibacterial performance is also influenced by the interaction between the polymer matrix and surrounding fluids. The hydrophilic nature of PVA/HPMC enables water absorption and matrix swelling, which may facilitate the diffusion of Zn^{2+} ions from embedded ZnO nanoparticles into the surrounding medium. Likewise, ROS may be generated at the ZnO surface under appropriate conditions, potentially contributing to localized antibacterial activity. These proposed mechanisms are consistent with previous reports on ZnO/polymer nanocomposites.

It is important to note, however, that the release kinetics of Zn^{2+} ions and ROS were not directly measured in this study. Therefore, although the observed inhibition zones clearly demonstrate the antibacterial effectiveness of the ZnO-incorporated fibers, the underlying antibacterial mechanisms and the duration of antimicrobial activity cannot be conclusively established based on the present experimental results. Accordingly, this work should be regarded as a proof-of-concept study demonstrating the feasibility of incorporating ZnO nanoparticles into PVA/HPMC electrospun fibers to obtain multifunctional wound dressing materials. Future investigations should include detailed analysis of cumulative release profiles and long-term antimicrobial performance under simulated physiological conditions to further elucidate the release behavior and validate the sustained activity of the system.

Overall, the incorporation of ZnO significantly enhanced the antibacterial performance of the PVA/HPMC electrospun fibers, while maintaining favorable structural, mechanical, and moisture-management properties. These combined characteristics suggest that the developed nanofibrous mats are promising candidates for wound dressing applications, particularly where antibacterial functionality is desired. Nevertheless, additional mechanistic studies and biological evaluations are required to fully validate their long-term performance and clinical potential.

The enhanced antibacterial activity observed in the PVA/HPMC/ZnO electrospun fibers can be attributed not only to the intrinsic properties of ZnO nanoparticles but also to the synergistic role of the polymer matrix. The PVA/HPMC system provides a highly hydrophilic and porous structure, which facilitates effective interaction with bacterial cells and promotes the diffusion of antibacterial agents, including Zn^{2+} ions. In addition, the uniform dispersion of ZnO nanoparticles within the polymer matrix helps prevent particle agglomeration, thereby maximizing the effective surface area available for antibacterial action. Furthermore, the swelling behavior of the PVA/HPMC matrix enhances moisture retention, which is beneficial for wound healing and improves the contact between antibacterial agents and bacterial cells. These combined effects contribute to the improved antibacterial performance of the composite fibers.

Regarding biocompatibility, although not directly evaluated in this study, previous reports have demonstrated that both the polymer matrix and ZnO nanoparticles exhibit favorable safety profiles for biomedical applications. Polyvinyl alcohol (PVA) is widely recognized as a biocompatible, non-toxic, and hydrophilic polymer suitable for wound dressing and tissue engineering applications [37].

Table 1. The antibacterial activity of PVA/HPMC based with 0-5% (w/w) of ZnO against *E. coli* and *S. aureus.*

Sample	*E. coli* [mm]	*S. aureus* [mm]
PVA/HPMC (blank)	0	0
PVA/HPMC/ 0.5% (w/w) of ZnO	9.00 ± 1.27	13.75 ± 0.65
PVA/HPMC/ 1% (w/w) of ZnO	9.51 ± 1.12	15.25 ± 2.63
PVA/HPMC/ 2% (w/w) of ZnO	10.01 ± 2.45	15.75 ± 1.94
PVA/HPMC/ 3% (w/w) of ZnO	10.13 ± 1.75	17.13 ± 1.03
PVA/HPMC/ 5% (w/w) of ZnO	13.00 ± 0.79	17.88 ± 0.25
+Ctrl (Gentamicin)	19.75 ± 1.09	21.00 ± 0.82

Table 2. Table showing the tensile properties of electrospun fibrous mats with different ZnO loading.

Sample	Tensile strength [MPa]	Young modulus [MPa]	Elongation [%]
PVA/HPMC/ 0% (w/w) of ZnO	3.93 ± 0.23	0.97 ± 0.18	10.60 ± 1.02
PVA/HPMC/ 0.5% (w/w) of ZnO	5.45 ± 0.59	1.15 ± 0.15	11.25 ± 1.32
PVA/HPMC/ 1% (w/w) of ZnO	5.64 ± 0.33	1.31 ± 0.20	12.30 ± 2.10
PVA/HPMC/ 2% (w/w) of ZnO	6.57 ± 0.53	1.63 ± 0.16	11.40 ± 0.76
PVA/HPMC/ 3% (w/w) of ZnO	7.99 ± 0.71	1.64 ± 0.11	14.86 ± 1.12
PVA/HPMC/ 5% (w/w) of ZnO	10.15 ± 1.02	1.91 ± 0.33	18.85 ± 0.83

Similarly, HPMC-based systems have been reported to possess biocompatibility, appropriate swelling behavior, and suitability for wound dressing applications [38]. ZnO nanoparticles have also been extensively studied for biomedical use, where their antibacterial activity is accompanied by acceptable bio-compatibility at controlled concentrations. For example, ZnO-incorporated PVA-based nanocomposite dressings have demonstrated high cell viability and cytocompatibility, supporting their application in wound healing [39]. In addition, hybrid ZnO/polymer systems have been shown to support cell attachment and proliferation without significant toxicity, while maintaining strong antibacterial activity [40].

Furthermore, recent open-access studies on ZnO-containing PVA-based composites report non-cytotoxic behavior and enhanced tissue regeneration, confirming their safety in wound healing applications [41]. Therefore, the combination of ZnO nanoparticles with PVA/HPMC matrices is expected to provide a safe and effective platform for wound healing applications, although further in vitro and in vivo biocompatibility studies are recommended for future work.

3.2.6 Mechanical properties of PVA/HPMC/ZnO electrospun fibers

The mechanical properties of PVA/HPMC nanofibers reinforced with varying concentrations of ZnO nanoparticles (0% to 5% (w/w) of ZnO) were evaluated through uniaxial tensile testing. The results demonstrate a clear enhancement in both stiffness and ductility with increasing ZnO content. Young's modulus increased from 0.971 MPa (pure PVA/HPMC) to 1.906 MPa at 5% (w/w) of ZnO, while tensile strength improved from 3.933 MPa to 10.154 MPa. These values fall within the desirable range for wound dressing applications, where moderate mechanical strength is essential to provide structural support without compromising flexibility. Furthermore, elongation at break rose from 10.601% to 18.849%, reflecting improved resilience and the ability of the mats to adapt to skin movement and irregular wound geometries.

The toughness of the materials defined as the area under the stress–strain curve increased notably with ZnO incorporation, indicating greater energy absorption before failure. This improvement is primarily attributed to strong hydrogen bonding interactions between the hydroxyl groups in PVA and HPMC and the surface of ZnO nanoparticles [21]. These interactions act as physical crosslinking points that enhance matrix cohesion and facilitate more effective stress transfer across the fiber network [22]. Additionally, the rigid and nanoscale structure of ZnO may restrict polymer chain mobility and may help distribute applied loads more uniformly, reinforcing the material. This synergy between physical reinforcement and dynamic bonding explains the observed mechanical improvements.

It should be noted that the mechanical testing in this study was performed under dry conditions. In physiological or wound environments, moisture absorption and swelling can significantly influence the mechanical performance of the dressing. Fluid uptake leads to plasticization of the polymer matrix, reducing intermolecular interactions such as hydrogen bonding and thereby decreasing stiffness and tensile strength. At the same time, increased chain mobility may enhance flexibility and extensibility, improving conformability to irregular wound surfaces. However, excessive swelling may weaken structural integrity, potentially compromising durability during handling and prolonged application. In addition, the presence of exudate and repeated hydration–dehydration cycles may further affect the stability and mechanical reliability of the fibrous network over time. Therefore, evaluating mechanical properties under wet or simulated physiological conditions is essential to ensure optimal performance in practical wound environments.

Nevertheless, the dry-state results provide an important baseline, demonstrating enhanced strength, toughness, and elongation at break with increasing ZnO content, indicating good structural support and flexibility. Future studies will include mechanical testing under wet or simulated physiological conditions to confirm the dressing's integrity and conformability during actual use.

Together, the enhanced strength, flexibility, and toughness demonstrate that ZnO-reinforced PVA/HPMC nanofibers possess the mechanical reliability necessary for practical wound dressing applications. These materials can withstand handling and application stresses while conforming comfortably to the wound site, promoting both user comfort and protective performance.

3.2.7 Potential application in wound management

The suitability of the developed PVA/HPMC/ZnO fibrous mats for specific wound types can be inferred from their physicochemical and functional properties. The swelling ratio (22% to 79%) indicates a moderate fluid absorption capacity, which is appropriate for managing low- to moderate-exudate wounds. These types of wounds are characterized by limited to intermediate levels of fluid production, including superficial wounds, abrasions, minor burns, surgical incisions, and partial-thickness wounds. In such cases, maintaining a moist environment is essential to promote healing processes such as cell migration, angiogenesis, and ECM formation, while preventing excessive fluid accumulation that may lead to tissue maceration. Materials with moderate swelling capacity are particularly suitable, as they can absorb excess exudate without becoming oversaturated or compromising structural integrity. In contrast, highly exuding wounds, such as chronic ulcers or heavily infected wounds, typically require dressings with significantly higher absorption capacity, such as super-absorbent electrospun fibrous mats or multilayer composite systems.

The contact angle values (18° to 43°) demonstrate relatively high hydrophilicity, facilitating effective fluid interaction and supporting a moist wound environment, which is known to accelerate tissue regeneration. Additionally, the improved mechanical properties, including enhanced tensile strength and elongation at break, ensure sufficient flexibility and durability for conformal contact with irregular wound surfaces, making the material suitable for dynamic skin regions and mechanically sensitive wound sites.

From a biological perspective, the electrospun fibrous structure, combined with moderate swelling and nanoscale surface roughness, provides a microenvironment that mimics the ECM, which is beneficial for cell attachment, proliferation, and tissue remodeling. Moreover, the incorporation of ZnO nanoparticles imparts antibacterial activity, reducing the risk of infection and supporting a favorable healing environment.

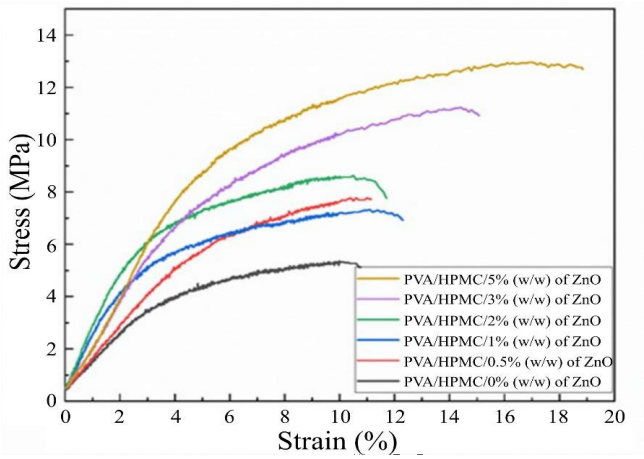


Figure 13. Tensile stress–strain curves of PVA/HPMC/0% (w/w) of ZnO, PVA/HPMC/0.5% (w/w) of ZnO, PVA/HPMC/1% (w/w) of ZnO, PVA/HPMC/2% (w/w) of ZnO, PVA/HPMC/3% (w/w) of ZnO, and PVA/HPMC/5% (w/w) of ZnO.

Overall, these combined properties suggest that the developed nanofibrous mats are particularly well-suited for low- to moderate-exudate wounds, where a balance between moisture retention, fluid absorption, mechanical integrity, and antimicrobial protection is required. However, further in vivo and clinical studies are necessary to validate their performance across different wound types.

4. Conclusion

In this study, PVA/HPMC-based electrospun fibers containing ZnO nanoparticles (0% to 5% (w/w)) were successfully fabricated and evaluated as multifunctional wound dressing ma-terials. The incorporation of ZnO was successfully achieved within the polymer matrix, pro-ducing uniform, bead-free nanofibers with enhanced surface roughness and improved physi-cochemical properties.

ZnO incorporation significantly improved the functional performance of the electro-spun mats. The swelling capacity increased with ZnO content, reaching 78.82 ± 1.55% at 5% (w/w), which is suitable for maintaining a moist wound environment and managing low- to moderate-exudate wounds. Mechanical testing demonstrated notable improvements in tensile strength, Young's modulus, and elongation at break, indicating enhanced structural stability and flexibility. In addition, the ZnO-loaded fibers exhibited significant antibacterial activity against both Staphylococcus aureus and Escherichia coli, highlighting their potential for re-ducing bacterial contamination in wound environments.

Overall, the developed PVA/HPMC/ZnO nanofibrous mats successfully combine moisture management, mechanical robustness, and antibacterial functionality within a single platform. These characteristics align with the requirements of modern wound dressings and demonstrate promising potential for practical wound care applications, particularly where in-fection prevention, structural integrity, and patient comfort are important considerations.

Nevertheless, some limitations should be acknowledged. Water vapor transmission rate (WVTR), cytotoxicity, biocompatibility, in vivo wound healing performance, long-term stability, and the release behavior of bioactive species were not investigated in the present study. Therefore, future studies should focus on biological evaluation, long-term perfor-mance, release behavior, and comparisons with commercially available wound dressings to further support clinical translation and practical implementation.

Acknowledgement

This work was financially supported by the Kasetsart University Institute for Advanced Studies (KUIAS) and Kasetsart University Research and Development Institute (KURDI, (FF(KU)51.69). The authors would also like to acknowledge the Department of Materials Engineering, Faculty of Engineering, Kasetsart University, for providing equipment and technical support. Special recognition is extended to Benjaporn Inseemeesak and Jirayu Kongtip for their invaluable contributions in refining the manuscript's content and presentation.

References

[1] H. Ragupathi, M. M. Pushparaj, S. M. Gopi, D. K. Govindarajan, and K. Kandaswamy, "Biofilm matrix: a multifaceted layer of biomolecules and a defensive barrier against antimicrobials," *Archives of Microbiology*, vol. 206, no. 11, p. 432, 2024.

[2] R. S.-Y. Wong, T. Tan, A. S.-R. Pang, and D. K. Srinivasan, "The role of cytokines in wound healing: from mechanistic insights to therapeutic applications," *Exploration of Immunology*, vol. 5, p. 1003183, 2025.

[3] J. G. Powers, L. M. Morton, and T. J. Phillips, "Dressings for chronic wounds," *Dermatologic Therapy*, vol. 26, no. 3, pp. 197–206, 2013.

[4] D. C. Aduba, and H. Yang, "Polysaccharide fabrication platforms and biocompatibility assessment as candidate wound dressing materials," *Bioengineering*, vol. 4, no. 1, p. 1, 2017.

[5] F. Jonidi Shariatzadeh, S. Currie, S. Logsetty, R. Spiwak, and S. Liu, "Enhancing wound healing and minimizing scarring: A comprehensive review of nanofiber technology in wound dressings," *Progress in Materials Science*, vol. 147, p. 101350, 2025.

[6] M. S. Ahmed, S. Yun, H.-Y. Kim, S. Ko, M. Islam, and K.-W. Nam, "Hydrogels and microgels: Driving revolutionary innovations in targeted drug delivery, strengthening infection management, and advancing tissue repair and regeneration," *Gels,* vol. 11, no. 3, p. 179, 2025.

[7] M. Ribeiro, M. Simões, C. Vitorino, and F. Mascarenhas-Melo, "Hydrogels in cutaneous wound healing: Insights into characterization, properties, formulation and therapeutic potential," *Gels,* vol. 10, no. 3, p. 188, 2024.

[8] M. P. Ferraz, "Wound dressing materials: Bridging material science and clinical practice," *Applied Sciences*, vol. 15, no. 4, p. 1725, 2025.

[9] J.-C. Park, T. Ito, K.-O. Kim, K.-W. Kim, B.-S. Kim, M.-S. Khil, H.-Y. Kim, and I.-S. Kim, "Electrospun poly(vinyl alcohol) nanofibers: Effects of degree of hydrolysis and enhanced water stability," *Polymer Journal*, vol. 42, no. 3, pp. 273–276, 2010.

[10] Y. Zhou, Q. Dong, H. Yang, X. Liu, X. Yin, Y. Tao, Z. Bai, and W. Xu, "Photocrosslinked maleilated chitosan/methacrylated poly(vinyl alcohol) bicomponent nanofibrous scaffolds for

use as potential wound dressings," *Carbohydrate Polymers*, vol. 168, pp. 220–226, 2017.

[11] R.-A. Vlad, A. Pintea, C. Pintea, E.-M. Redai, P. Antonoaea, M. Birsan, and A. Ciurba, "Hydroxypropyl methylcellulose-A key excipient in pharmaceutical drug delivery systems," *Pharmaceutics*, vol. 17, no. 6, p. 784, 2025.

[12] N. Palani, P. Vijayakumar, P. Monisha, S. Ayyadurai, and S. Rajadesingu, "Electrospun nanofibers synthesized from polymers incorporated with bioactive compounds for wound healing," *Journal of Nanobiotechnology*, vol. 22, no. 1, p. 211, 2024.

[13] Y. Wang, J. Liu, T. Wang, L.-Z. Liu, C. Tian, Y. Cui, W. Shao, X. Hua, Y. Shi, and Y. Wang, "Antibacterial properties and mechanism of nanometer zinc oxide composites," *Food Packaging and Shelf Life*, vol. 40, p. 101167, 2023.

[14] C. R. Mendes, G. Dilarri, C. F. Forsan, V. de. Moraes, R. Sapata, P. R. M. Lopes, P. B. de. Moraes, R. N. Montagnolli, H. Ferreira, and E. D. Bidoia, "Antibacterial action and target mechanisms of zinc oxide nanoparticles against bacterial pathogens," *Scientific Reports*, vol. 12, no. 1, p. 2658, 2022.

[15] B. da Silva, M. P. Abucafy, E. B. Manaia, J. A. O. Junior, B. G. Chiari-Andreo, R. C. R. Pietro, and L. A. Chiavacci, "Relationship between structure and antimicrobial activity of zinc oxide nanoparticles: An overview," *International Journal of Nanomedicine*, vol. 14, pp. 9395–9410, 2019.

[16] P. P. Mahamuni-Badiger, P. M. Patil, M. V. Badiger, P. R. Patel, B. S. Thorat-Gadgit, A. Pandit, and R. A. Bohara, "Biofilm formation to inhibition: Role of zinc oxide-based nanoparticles," *Materials Science and Engineering: C*, vol. 108, p. 110319, 2020.

[17] L. K. Sellappan, and S. Manoharan, "Fabrication of bioinspired keratin/sodium alginate based biopolymeric mat loaded with herbal drug and green synthesized zinc oxide nanoparticles as a dual drug antimicrobial wound dressing," *International Journal of Biological Macromolecule*s, vol. 259, p. 129162, 2024.

[18] S. Manoharan, P. Balakrishnan, and L. K. Sellappan, "Fabrication of highly flexible biopolymeric chitosan/agarose based bioscaffold with Matricaria recutita herbal extract for antimicrobial wound dressing applications," *International Journal of Biological Macromolecules*, vol. 281, p. 136195, 2024.

[19] L. K. Sellappan, S. Mishra, S. Sundaresan, T. Rathinavelan, and S. Majumdar, "Multifunctional NiO-curcumin nanocomposite-loaded chitosan-alginate scaffolds for enhanced bone tissue regeneration and antibacterial activity," *Journal of Drug Delivery Science and Technology*, vol. 110, p. 107114, 2025.

[20] K. P. Greeshma, S. Muthulingam, R. Thamizselvi, and D. B. Sen, "Antimicrobial studies and characterization of ZnO nanoparticles by chemical method," *GSC Advanced Research and Reviews*, vol. 8, pp. 071-077, 2021.

[21] G. Nagaraju, G. C. Shivaraju, G. Banuprakash, and D. Rangappa, "Photocatalytic activity of ZnO nanoparticles: Synthesis via solution combustion method," *Materials Today: Proceedings*, vol. 4, pp. 11700–11705, 2017.

[22] R. Kumar, A. Umar, G. Kumar, and H. S. Nalwa, "Antimicrobial properties of ZnO nanomaterials: A review," *Ceramics International*, vol. 43, no. 5, pp. 3940–3961, 2017

[23] B. Qu, Z. Xiao, and Y. Luo, "Sustainable nanotechnology for food preservation: Synthesis, mechanisms, and applications of zinc oxide nanoparticles," *Journal of Agriculture and Food Research*, vol. 19, p. 101743, 2025.

[24] S. -E. Jin, and H.-E. Jin, "Antimicrobial activity of zinc oxide nano/microparticles and their combinations against pathogenic microorganisms for biomedical applications: From physico-chemical characteristics to pharmacological aspects," *Nanomaterials*, vol. 11, no. 2, p. 263, 2021.

[25] U. Pal, C. Kim, N. Jadhav, and Y. Kang, "Ultrasound-assisted synthesis of mesoporous ZnO nanostructures of different porosities," *Journal of Physical Chemistry C*, vol. 113, pp. 14676–14680, 2009.

[26] S. Jiang, K. Lin, and M. Cai, "ZnO nanomaterials: Current advancements in antibacterial mechanisms and applications," *Frontiers in Chemistry*, vol. 8, p. 580, 2020.

[27] V. Sethi, M. Kaur, A. Thakur, P. Rishi, and A. Kaushik, "Unravelling the role of hemp straw derived cellulose in CMC/PVA hydrogel for sustained release of fluoroquinolone antibiotic," *International Journal of Biological Macromolecules*, vol. 222, pp. 844–855, 2022.

[28] I. M. Jipa, A. Stoica, M. Stroescu, L.-M. Dobre, T. Dobre, S. Jinga, and C. Tardei, "Potassium sorbate release from poly(vinyl alcohol)-bacterial cellulose films," *Chemical Papers*, vol. 66, pp. 138–143, 2012.

[29] P. Mondal, M. Mondal, J. Chakraborty, N. Sing, B. Ghosh, S. Ray, K. Mahali, "Advances in upcycling waste cellulose into functional materials: Strategies, challenges, and emerging applications—A comprehensive review," *Next Research*, vol. 2, no. 4, p. 100768, 2025.

[30] C. Aumnate, N. Soatthiyanon, T. Makmoon, and P. Potiyaraj, "Polylactic acid/kenaf cellulose biocomposite filaments for melt extrusion based-3D printing," *Cellulose*, vol. 28, pp. 8509–8525, 2021.

[31] U. Ejaz, R. Rashid, S. Ahmed, K. K. Narejo, A. Qasim, M. Sohail, S. T. Ali, J. T. Althakafy, A. K. Alanazi, H. M. Abo-Dief, and S. F. Moin, "Synthesis of methylcellulose-polyvinyl alcohol composite, biopolymer film and thermostable enzymes from sugarcane bagasse," *International Journal of Biological Macromolecules*, vol. 235, p. 123903, 2023.

[32] F. Van den Berg, "Extracellular matrix," in *Fascia: The Tensional Network of the Human Body*, R. Schleip, T. W. Findley, L. Chaitow, and P. A. Huijing, Eds. Oxford: Churchill Livingstone, 2012, pp. 165–170.

[33] L. Li, K. Crosby, M. Sawicki, L. L. Shaw, and Y. Wang "Effects of surface roughness of hydroxyapatite on cell attachment and proliferation," *Journal of Biotechnology & Biomaterials*, vol. 2, p. 150, 2012.

[34] M. J. Dalby, N. Gadegaard, R. Tare, A. Andar, M. O. Riehle, P. Herzyk, C. D. W. Wilkinson, and R. O. C. Oreffo, "The control of human mesenchymal cell differentiation using nanoscale symmetry and disorder," *Nature Materials*, vol. 6, no. 12, pp. 997–1003, 2007.

[35] E. S. Place, N. D. Evans, and M. M. Stevens, "Complexity in biomaterials for tissue engineering," *Nature Materials*, vol. 8, no. 6, pp. 457–470, 2009.

[36] K. Menzies, and L. Jones, "The impact of contact angle on the biocompatibility of biomaterials," *Optometry and Vision Science*, vol. 87, pp. 387–399, 2010.

[37] J. A. Ortiz, F. A. Sepulveda, S. Flores, M. Saavedra, S. Saez-Silva, T. Jimenez, P. Murgas, S. Troncoso, C. Sanhueza, M. T. Ulloa, L. P. Torre, M. Ahumada, T. Corrales, H. Palza, and P. A. Zapata, "Electrospun polyvinyl alcohol/sodium alginate nanocomposite dressings loaded with ZnO and bioglass: Characterization, antibacterial activity, and cytocompatibility," *Polymers*, vol. 17, no. 16, p. 2185, 2025,

[38] L. Ding, Q. Qi, S. Zhang, C. Ren, M. Deng, Z. Sun, R. Zhang, Q. Liu, S. Duan, X. Wang, and L. Wang "Hydroxypropyl methylcellulose reinforced collagen/ PVA composite hydrogel wound dressing with self-adaptive, hemostasis and antibacterial ability for wound healing," *International Journal of Biological Macromolecules*, vol. 304, pt. 2, p. 140811, 2025.

[39] J. A. Ortiz, F. A. Sepulveda, S. Flores, M. Saavedra, S. Saez-Silva, T. Jimenez, P. Murgas, S. Troncoso, C. Sanhueza, M. T. Ulloa, L. P. Torre, M. Ahumada, T. Corrales, H. Palza, and P. A. Zapata, "Electrospun polyvinyl alcohol/sodium alginate nanocomposite dressings loaded with ZnO and bioglass: Characterization, antibacterial activity, and cytocompatibility," *Polymers*, vol. 17, no. 16, p. 2185, 2025.

[40] R. M. Abdel-Rahman, J. Frankova, R. Sklenarova, L. Kapralkova, I. Kelnar, and A. M. Abdel-Mohsen, "Hyaluronan/zinc oxide nanocomposite-based membrane: Preparation, characterization, and in vitro and in vivo evaluation*," ACS Applied Polymer Materials*, vol. 4, no. 10, pp. 7723–7738, 2022.

[41] S. Reiisi, N. Khalighi, S. Akkoc, and S. Shirian, "Biocompatible ZnO nanoflower-infused chitosan/alginate/PVA composite for accelerated skin regeneration," *Journal of Materials Science: Materials in Medicine*, vol. 36, no. 1, p. 87, 2025.